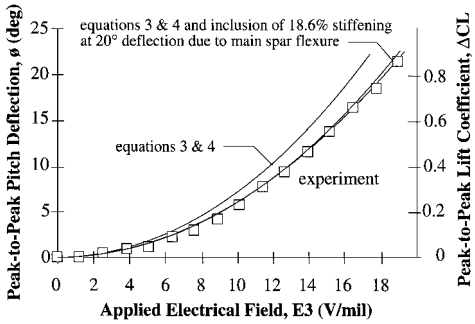

Fig. 4 Static pitch deflection with applied field.

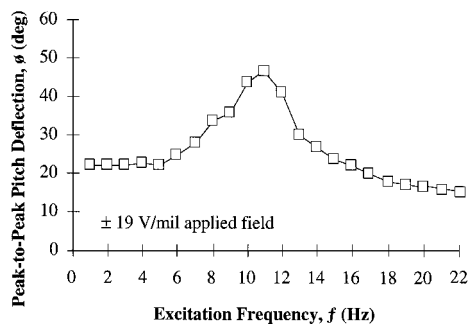

Fig. 5 Tip-joint Flexspar dynamic pitch deflection characteristics at ±19 V/mil.

Because of the mass balancing and collocation of the hinge line and aerodynamic center aeroelastic coupling and flutter were not detected. Figure 4 shows the static bench and wind-tunnel results.

From Fig. 4, it is clear that if the added stiffness of the main spar is included, then the error between theory and experiment drops to under 2%.

Following static testing, dynamic tests were conducted to determine the frequency response of the actuator. Figure 4 shows a natural frequency of approximately 11 Hz, and the break frequency of 23 maximum power consumption recorded during these tests was 40 mW.

The data of Figs. 4 and 5 clearly show that the tip-joint Flexspar generates very high deflections for given actuation potentials. The blunted peak at the natural frequency of approximately 11 Hz is caused by the shell bumping against the stops, which were set to approximately ±22 deg. From Fig. 4, the lift-curve slope may be resolved to approximately 0.039/deg. The low value of lift curve slope is primarily due to a significant amount of aerodynamic relieving that occurred at the base of the mount.

Conclusions

This study has shown that laminated plate theory and kinematics can successfully predict the deflections generated by piezoceramic Flexspar flight control surface actuators. Experimental model testing showed that pitch deflections up to ±11 deg may be achieved with Flexspar control surfaces measuring 4 in. in span with a 3.33-in. mean geometric chord. Dynamic testing demonstrated an 11-Hz natural frequency and a 23-Hz break frequency with 40 mW of power consumed at the most extreme actuation condition.

Acknowledgments

The authors would like to acknowledge the Auburn University School of Engineering and Aerospace Engineering Department for supporting this research, along with Brian Chin and the Auburn University Materials Engineering Program. The authors would also like to thank Clifton Minter, Steven Williams, and Steven Rose for helping with the construction of the Flexspar fins.

References

[1]Crawley, E. F., Lazarus, K. B., and Warkentin, D. J., "Embedded Actuation and Processing in Intelligent Materials," 2nd International Workshop on Composite Materials and Structures (Troy, NY), Army Research Office, Research Triangle Park, NC, Sept. 1982.

[2]Ehlers, S. M., and Weisshaar, T. A., "Static Aeroelastic Behavior of an Adaptive Laminated Piezoelectric Composite Wing," *AIAA Journal*, Vol. 28, No. 4, 1990, pp. 1611–1623.

[3]Barrett, R., Gross, R. S., and Brozoski, F., "Missile Flight Control Using Active Flexspar Actuators," *Proceedings of the Society of Photo-Optical Instrumentation Engineers 1995 Smart Structures and Materials Conference* (San Diego, CA), Vol. 2443, Society of Photo-Optical Instrumentation Engineers, Bellingham, WA, 1995, pp. 52–61.

[4]Jones, R. M., "Micromechanical Behavior of a Lamina," *Mechanics of Composite Materials*, Hemisphere, New York, 1975, pp. 147–237.

R. K. Kapania
Associate Editor

Interface Wavelength Between Confined Supersonic Two-Dimensional Jets and Subsonic Streams

Lawrence J. De Chant,* Jerald A. Caton,† and Malcolm J. Andrews‡
Texas A&M University, College Station, Texas 77843

Nomenclature

A = cross-sectional area
g = gravitational constant
H_s = splitter plate height
M = Mach number
P = total pressure
p = static pressure
T = temperature
U = free/mainstream velocity
u = streamwise velocity
v = cross-stream velocity
x = streamwise coordinate
β = $(M^2 - 1)^{1/2}$
γ = ratio of specific heats
ε = small perturbation term, $1 - U_1/U_{1s}$
ξ = dimensionless interface amplitude, $(\beta_{1s})^2[1 - U_1/U_{1s}]$
ρ = density
ϕ = small disturbance velocity potential

Subscripts

c = critical
eff = effective state
s = streamline value
0 = stagnation or reservoir condition
1, 2 = primary and secondary streams

Introduction

A MODEL for the freejet interface wavelength of an inviscid, supersonic and subsonic stream is described. The model, which is a confined flow extension to a previous methodology, involves modifying the lowest-order perturbation quantities to honor internal flow conservation and to provide the first critical location of the slipline. We show reasonable agreement between the model and analog measurements for the critical wavelength.

Received Dec. 20, 1996; revision received March 27, 1997; accepted for publication April 10, 1997.

*Graduate Research Assistant, Department of Mechanical Engineering, MS 3123.

†Professor, Department Head, Department of Mechanical Engineering, MS 3123. Member AIAA.

‡Assistant Professor, Department of Mechanical Engineering, MS 3123. Member AIAA.

Supersonic ejector nozzles are of considerable interest for aeropropulsion applications because of their noise suppression and improved performance capabilities. Indeed, the mixed jet issuing from a core/ejector propulsion system combination is the primary source of noise generation from airplanes at takeoff.[1] Although freejets are a useful limiting form of the ejector flow, the effect of confinement on the flowfield is important, because confinement strongly influences the subsonic and supersonic streams, as well as their interface. Moreover, a description of the inviscid flowfield structure within an ejector nozzle has design implications for acoustic, structural, and fluid mechanical considerations.

De Chant et al.[2] give formulas for the slipline wavelength for two-dimensional and axisymmetric, supersonic–subsonic jets in a subsonic stream. We extended their theory to include internal flows. The outcome is a general relationship that provides internal flowfield information for a supersonic ejector flowfield, inasmuch as the location of the first maximum expansion corresponds approximately to the location of the Fabri-choke.[3,4]

Theoretical Model

Figure 1 presents a schematic of the freejet problem following De Chant et al.[2] The principal parameter discussed is $x_c/2$, which is the dimensionless location of the first minimum in the expansion/compression system resulting in the flow. From De Chant et al.,[2] values for both axisymmetric and two-dimensional unconfined flows are described by Eq. (1) (axisymmetric) and Eq. (2) (two dimensional):

$$x_c/2 = 1.22\beta_{\text{eff}} - 0.22\beta_{1s} \equiv 1.22\left(1 + \tfrac{1}{2}\xi_n^{\frac{1}{2}}\right)\beta_{1s} - 0.22\beta_{1s} \quad (1)$$

$$x_c/2 = 2\beta_{\text{eff}} - \beta_{1s} \equiv 2\left(1 + \tfrac{1}{2}\xi_n^{\frac{1}{2}}\right)\beta_{1s} - \beta_{1s} \quad (2)$$

where $\beta_{1s} = (M_{1s}^2 - 1)^{1/2}$ and $\xi_n = (\beta_{1s})^2[1 - U_1/U_{1s}]$. By symmetry, half the length of the first critical is approximately the local maximum of the primary expansion and corresponds to the location of Fabri's aerodynamic choke. Figure 2 shows the confined jet problem.

Following the analysis developed by De Chant et al.,[2] the perturbation expansion is considered:

$$\frac{u}{U_{1s}} = 1 + \frac{\partial\phi}{\partial x}\varepsilon + \cdots \qquad \varepsilon \equiv \left(1 - \frac{U_1}{U_{1s}}\right) \quad (3)$$

where U_{1s} is the velocity at the interface. In Ref. 2, the slipline velocity U_{1s} was estimated using a static pressure matching methodology. We employ a complete control volume methodology to account for the internal flow effects. The approach considers the basic problem for an internal flow, namely, computing M_{1s}, M_{2s}, and U_{1s}.

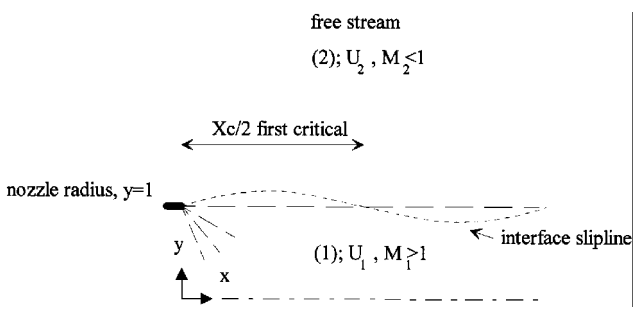

Fig. 1 Free jet geometry and definitions.

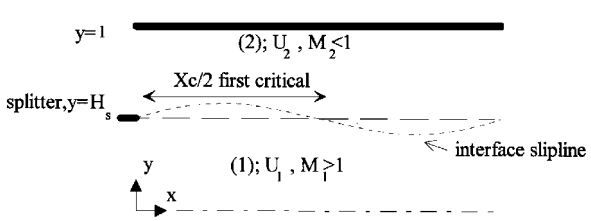

Fig. 2 Internal/ejector flow geometry and definitions.

The conditions for a freejet are based solely on local static pressure matching. Consequently, problems for $A_2/A_1 \gg 1$ are analyzed using static pressure and mass conservation. Unfortunately, the local one-dimensional control volume assumptions are poor approximations for sufficiently small area ratios, A_2/A_1. Therefore, we cannot expect to use this methodology for $A_2/A_1 \approx 1$. A more rigorous bound on the limiting area ratio is subsequently developed.

The governing equations for these two flows are mass conservation[5]

$$\left(\frac{M_1}{M_{1s}}\right)\left(\frac{\{1 + [(\gamma-1)/2]M_{1s}^2\}}{\{1 + [(\gamma-1)/2]M_1^2\}}\right)^{(\gamma+1)/2(\gamma-1)} + \left(\frac{A_2}{A_1}\right)\left(\frac{M_2}{M_{2s}}\right) \times \left(\frac{\{1 + [(\gamma-1)/2]M_{2s}^2\}}{\{1 + [(\gamma-1)/2]M_2^2\}}\right)^{(\gamma+1)/2(\gamma-1)} = 1 + \left(\frac{A_2}{A_1}\right) \quad (4)$$

and static pressure matching

$$\left(\frac{P_{01}}{P_{02}}\right) = \left(\frac{\{1 + [(\gamma-1)/2]M_{1s}^2\}}{\{1 + [(\gamma-1)/2]M_{2s}^2\}}\right)^{\gamma/(\gamma-1)} \quad (5)$$

These relationships provide closure for the internal flow Mach numbers and area ratios. The flow is locally assumed as isentropic, which gives the slipline velocity as

$$\frac{U_1}{U_{1s}} = \frac{M_1}{M_{1s}}\left(\frac{\{1 + [(\gamma-1)/2]M_{1s}^2\}}{\{1 + [(\gamma-1)/2]M_1^2\}}\right)^{\frac{1}{2}} \quad (6)$$

Equation (6) contains the freejet solution as a degenerate case when $A_2/A_1 \longrightarrow \infty$ giving the result of De Chant et al.[2]:

$$M_{1s}^2 = [2/(\gamma-1)]\left(\{1 + [(\gamma-1)/2]M_1^2\}(p_1/p_2)^{(\gamma-1)/\gamma} - 1\right) \quad (7)$$

With the low-order forms in Eqs. (4–6), the analysis proceeds by solving the preceding equations for the parameter M_{1s} and U_{1s} and then substituting into the critical length formula [Eq. (1) or (2)]. The solution of the nonlinear system has been conveniently performed using a version of Broyden's method,[6] a multivariable form of the secant method.

For any particular problem, an estimate of the minimum area ratio that is consistent with the control volume approximation is of interest. This may be obtained by combining Eqs. (4) and (5) to yield the single variable relationship $F(M_{2s})$,

$$F \equiv M_1\left(\frac{2}{\gamma-1}\left[\left(\frac{P_{01}}{P_{02}}\right)^{(\gamma-1)/\gamma}\left(1 + \frac{\gamma-1}{2}M_{2s}^2\right) - 1\right]\right)^{-\frac{1}{2}} \times \left(\frac{(P_{01}/P_{02})^{(\gamma-1)/\gamma}\{1 + [(\gamma-1)/2]M_{2s}^2\}}{\{1 + [(\gamma-1)/2]M_1^2\}}\right)^{(\gamma+1)/2(\gamma-1)} + \left(\frac{A_2}{A_1}\right)\left(\frac{M_2}{M_{2s}}\right)\left(\frac{\{1 + [(\gamma-1)/2]M_{2s}^2\}}{\{1 + [(\gamma-1)/2]M_2^2\}}\right)^{(\gamma+1)/2(\gamma-1)} - 1 - \left(\frac{A_2}{A_1}\right) = 0 \quad (8)$$

Equation (8) is posed in terms of M_{2s}, rather than M_{1s}, because M_{2s} is necessarily bounded by $M_2 < M_{2s} < 1$. This bounding permits a straightforward selection of an initial guess needed for the iterative solution of Eq. (8). Using these two constraints, the function F is readily searched to find a sign change that implies a possible solution. An alternative would be to demand the two conditions, $F = \partial F/\partial M_{2s} = 0$ and Eq. (8), and thereby solve for a critical area ratio and the critical M_{2s}. However, this adds another multiple variable problem that is less well posed due to the unknown critical area ratio.

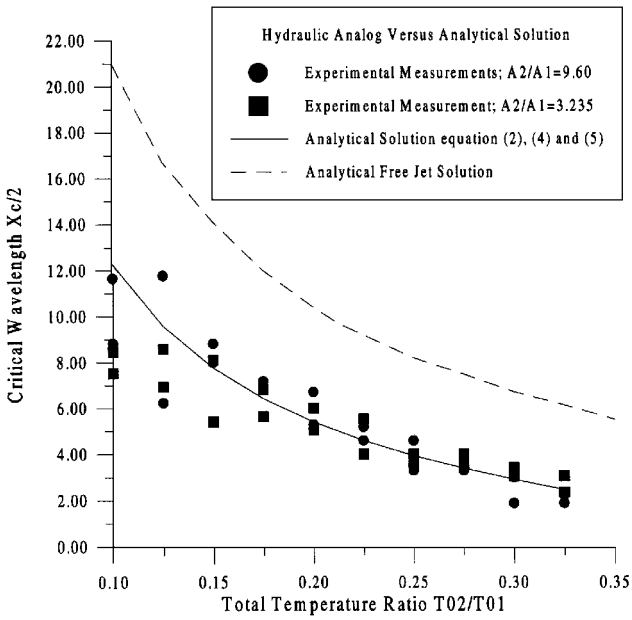

Fig. 3 Critical interface lengths.

Comparison of Model with Experimental Data

The key parameter x_c has been measured using the hydraulic analogy described by De Chant and Caton[7] and is presented in Fig. 3 for several area ratios and a Mach 2.0 primary stream interacting with a negligible secondary flow with fixed secondary total pressure and temperature. The area ratios associated with the measurements are large enough so that the pressure matching closure is suitable. Indeed, for the large area ratios considered, both the $A_2/A_1 = 9.60$ and $A_2/A_1 = 3.235$ analytical curves are virtually identical. As such, only a single combined curve is presented. So as not to leave the reader with the impression that this analysis is independent of area ratio, a freejet solution,[2] i.e., $A_2/A_1 \longrightarrow \infty$ is presented in Fig. 3 for comparison. It is apparent that the freejet wavelength is a poor approximation to the internal flow interface solution.

Additionally, to help assess the effect of experimental error, we ran a series of repeatability tests, using different reservoir ratios to assess the effect of initial reservoir ratio on the measurements. A significant but acceptable amount of error is introduced by varying this ratio, especially significant differences in reservoir height, i.e., T_{02}/T_{01} small, because three-dimensional effects are pronounced for these small total temperature ratios.

Conclusions

We have developed and compared to experimental hydraulic analog data inviscid, confined supersonic and subsonic stream interactions. Formulas for the first critical location of the slipline are derived. Reasonable agreement is shown between the extended, internal flow, theoretical model and experimental measurements. This work is of considerable interest to aerodynamic mixer ejector nozzle development, a potentially critical technology to the high-speed civil transport program.

References

[1]Champagne, G. A., "Jet Noise Reduction Concepts for the Supersonic Transport," AIAA Paper 91-3328, Sept. 1991.

[2]De Chant, L. J., Seidel, J. A., and Andrews, M. J., "Interface Wavelength Between Supersonic Jets and Subsonic Flowfields," *AIAA Journal*, Vol. 34, No. 9, 1996, pp. 1946–1948.

[3]Fabri, J., and Siestrunck, R., "Supersonic Air Ejectors," *Advances in Applied Mechanics*, Vol. 5, Academic, New York, pp. 1–34.

[4]Addy, A. L., Dutton, J. C., and Mikkelsen, C. D., "Supersonic Ejector-Diffuser Theory and Experiments," Dept. of Mechanical and Industrial Engineering, Engineering Experiment Station, Univ. of Illinois, UILU-ENG-82-400, Urbana, IL, Aug. 1981.

[5]Anderson, J. D., *Modern Compressible Flow*, McGraw–Hill, New York, pp. 120–128.

[6]Burden, R. L., and Faires, J. D., *Numerical Analysis*, PWS-Kent, Boston, 1993, pp. 560–566.

[7]De Chant, L. J., and Caton, J. A., "Measurement of Confined Supersonic, 2-d Jet Lengths Using the Hydraulic Analogy," *Experiments in Fluids* (submitted for publication).

S. Glegg
Associate Editor

k–ζ (Enstrophy) Compressible Turbulence Model for Mixing Layers and Wall Bounded Flows

G. A. Alexopoulos* and H. A. Hassan†
North Carolina State University, Raleigh, North Carolina 27695-7910

Introduction

THE objective of this work is to extend the k–ζ model of Robinson et al.[1] to compressible turbulent flows. The success of the k–ζ in reproducing a variety of incompressible flows should provide a good basis for the current model. As in the incompressible model, the current model will be based on the exact compressible equations to ensure that the correct physics is incorporated.

Compressible flows require for their description a velocity field and two thermodynamic variables, such as the density and temperature. Because of this, the fluctuations of these thermodynamic variables are as important as those of the velocity in determining the resulting turbulent flow. As a result, traditional two-equation and stress models[2] have proven to be inadequate in describing such flows. Therefore, it appears that an appropriate compressible turbulent flow model of the two-equation variety should include six equations that describe variances of velocity, density, temperature, and their respective dissipation rates.

A simplification of this approach can be achieved by using Morkovin's hypothesis.[3] According to this hypothesis, the pressure and total temperature fluctuations are small for nonhypersonic compressible boundary layers with conventional rates of heat transfer, i.e.,

$$p'/P \ll 1, \qquad T_0'/T_0 \ll 1 \tag{1}$$

As a result,

$$\rho'/\rho \simeq -T'/T \simeq (\gamma - 1)M^2(u'/U) \tag{2}$$

In this equation, p', T_0', ρ', T', and u' are the fluctuating pressure, total temperature, density, temperature, and velocity, respectively. Also, M is the Mach number and γ is the ratio of specific heats. The remaining variables represent mean properties. Based on Eq. (2), equations governing variances of turbulent quantities can be taken as the equation for the turbulent kinetic energy. However, equations governing the dissipation rates of the resulting variances may not be the same.

The approach employed in developing a k–ζ compressible model is to use the guidelines set in Ref. 1 to model the additional terms. Thus, for low Mach numbers, the new model reduces to that of Ref. 1. It is shown in Ref. 4 that when Morkovin's hypothesis is invoked, the effects of compressibility for flows considered here result in an additional term in the k equation, which is

$$-C_1(\rho k/\tau_\rho) \tag{3}$$

Received April 26, 1996; presented as Paper 96-2039 at the AIAA 27th Fluid Dynamics Conference, New Orleans, LA, June 17–20, 1996; revision received Feb. 17, 1997; accepted for publication March 1, 1997.

*Research Assistant, Mechanical and Aerospace Engineering. Student Member AIAA.

†Professor, Mechanical and Aerospace Engineering. Associate Fellow AIAA.